J. Agr. Sci. Tech. (2019) Vol. 21(6): 1607-1622

Relationship between Pedodiversity and Geomorphologic Patterns Using Modified Fractal Dimension (Case Study: East of Isfahan, Central Iran)

S. Havaee[1], N. Toomanian[2*], and A. Kamali[1]

ABSTRACT

Based on the obvious relationship between geoforms and soils, pedodiversity was investigated in this study through the Spatial Distribution Patterns (SDPs) of LandForms (LFs) using quantitative analysis of the irregular geometry of LFs in Zayandeh-Rud Valley. The main objectives of this research were to: (1) Assess the applicability of fractal and modified fractal dimensions in quantifying the irregular geometry of LFs in the study area and (2) Specify the relationship between the irregular geometry of LFs and the pedodiversity in the region. LF units were delineated using aerial photographs at a scale of 1:55,000; and the geoform classification system was defined according to Zinck. After fieldwork and soil sampling, Soil Taxonomy was used for soil classification at the family level and determination of the geomorphic map units. The fractal Dimension (D) and modified fractal Dimension (D_m), as geometric indicators, and richness (S), Shannon diversity index (H′), maximum diversity (H'_{max}), and Evenness (E), as pedodiversity measures, were determined for LFs. Results showed that *D* and D_m were appropriate indicators of geometric irregularity, with their high values corresponding to fluvial surfaces with intensive dissection and deposition processes, and their low values corresponding to the smoother and more stable landforms. Comparison of the pedodiversity indices with the geometric measures in the landscapes showed that D_m was a suitable alternative to *D* in presenting structure of landscapes with high *D* and D_m values relatively coinciding with high amounts of richness in the study area. In addition, D_m was more closely related to the diversity indices than *D* was to the discernment of the pedodiversity of LFs.

Keywords: Geoforms, Geometric irregularity, Landforms, Shannon diversity index.

INTRODUCTION

Evaluation of the spatial patterns of geomorphic and pedologic systems and their diversity is an essential step for conservation and management of the pedosphere. However, pedologic systems have complex shapes with irregular geometry, which makes it difficult to understand the spatial structures and distribution of these terrain sectors. In fact, one of the inherent properties of earth-surface systems is their irregular geometry (San José Martínez and Javier Caniego Monreal, 2013), whose characterization is necessary to determine the spatial pattern of the earth-surface systems. This irregular geometry is easy to see but difficult to quantify via Euclidean geometry. Fractal geometry provides mathematical tools to characterize the complex geometry of irregular shapes in nature (Anderson *et al*., 2006; Burrough, 1981; San José Martínez and Javier Caniego Monreal, 2013).

[1] Department of Soil Science, College of Agriculture, Vali-e-Asr University, Postal Code 7713936417, Rafsanjan, Islamic Republic of Iran.
[2] Department of Soil and Water Research, Isfahan Agricultural and Natural Resources Research and Education Center, AREEO, Isfahan, Islamic Republic of Iran.
[*] Corresponding author; e-mail: norairtoomanian@gmail.com

[DOR: 20.1001.1.16807073.2019.21.6.6.5]

A fractal Dimension (D) that Mandelbrot (1982) proposed can be derived from a power law model of the relationships between generator components of a fractal object, i.e. polygon delineation. A fractal dimension can reflect the irregularity of a fractal object (Mandelbrot, 1982). For example, the *D* value of a more irregular coastline is higher than the *D* value for a smooth one (Mandelbrot, 1967). Therefore, *D* can be used to quantify and contour the irregular geometry of fractal shapes (Anderson *et al*., 2006).

If the delineation of a geomorphic unit is assumed as a subset of points in two-dimensional space, *D* can be obtained from a power law model based on the self-similar hypothesis of the spatial distribution of geoform type abundance (Ibáñez *et al*., 2009). Ibáñez *et al*. (2009) introduced *D* as a measure of the irregularity of soil map units. In this way, *D* has been used as a mathematical tool to characterize the irregular geometry of earth-surface systems (such as landscapes and soilscapes) and is related to the diversity of a landscape. For example, in an analysis of a soilscape, Saldaña *et al*. (2011) used *D* as a measure of the diversity of soil map units. In that study, old LFs (LFs are geomorphic units with constant soil forming factors) dismantled by short creek and gully incisions in Rañas and high terraces had complex shapes and thus high fractal dimensions. In contrast, more stable landforms exhibited lower fractal dimension values. Their results showed that *D* is a good indicator of soilscape evolution and terrain stability. In addition, several other valuable studies about applying *D* to investigate the spatial distribution of soilscapes and landscapes exist (Ibáñez *et al*., 2005; Ibáñez *et al*., 2009; Ibáñez *et al*., 2013; Martin and Rey, 2000; Parsons, 2000; Saldana, 2013; Saldaña and Ibáñez, 2004; Saldaña *et al*., 2011).

Area-perimeter relations are used to consider the irregular geometry of fractal objects (Lam, 1990; Mandelbrot, 1982; Saldaña *et al*., 2011). Burrough (1981) used the natural log of one-fourth the perimeter against the natural log of the area to calculate the fractal dimension. In that approach, the number of image elements in a given delineation is counted as the Area (A) and the length of the delineation's boundary serves as the Perimeter (P) (Lovejoy and Mandelbrot, 1985).

About two decades ago, Olsen *et al*. (1993) introduced a modified fractal dimension (D_m) to assess landscape structure. They stated that the management of natural resources and environmental factors requires determination of the spatial dynamics of diversity within a landscape, not just the general diversity of the landscape. They believed the shape of a patch is not the only factor that affects diversity within a landscape and the juxtaposition of a given patch to other patches also has significant effects (Olsen *et al*., 1993).

The concept of diversity has two main components: the number of different entities (richness) and their relative abundance (evenness) (Ibáñez *et al*., 1995). It is clear that a uniform distribution of various classes leads to maximum values of evenness and subsequently higher diversity. In the same vein, a greater variety of species means higher diversity (Ibáñez *et al*., 1995). Therefore, D_m accounts for patch richness and patch evenness in association with fractal dimension. Figures 1 and 2 illustrate this point via simple examples. Patches can be the map delineations of landforms, or pedotaxa.

Cases I and II are two hypothetical landscapes. Case (I) has cells of only two patch classes (the background (blank areas) and a). Case (II) has cells of five patch classes (the background, a, b. c, and d). Both cases yield the same fractal dimension because their geometry is identical (only the calculation for case (II) is shown because its patches are easily distinguished). The class variability shown in Figure 1 is not due to geometry. In this case, the fractal dimension does not distinguish the patch variability resulting from patch classification. According to Figure 1, in Case I the

[DOR: 20.1001.1.16807073.2019.21.6.6.5]

Case I

a	a		a	a
a	a		a	a
a	a		a	a
a	a		a	a

Case II

a	a		b	b
a	a		b	b
c	c		d	d
c	c		d	d

Patch	P	A	D
a	8	4	1
b	8	4	1
c	8	4	1
d	8	4	1
Background	20	9	1.46

Figure 1. Two landscapes that are indistinguishable using the simple fractal calculation from the equation $P = k \times \sqrt[2]{A^D}$ (Adapted from Olsen *et al*., 1993).

a	a	c	b
a	a	c	b
c	c	b	b
c	c	g	b

Patch	Class	*A*	*P*	*D*	D_m
1	a	4	8	1.00	1.14
2	c	2	6	1.16	1.43
3	b	5	12	1.36	1.58
4	c	4	8	1.00	1.40
5	g	1	4	1.00	1.00

Figure 2. Example calculation comparing *D* and D_m (Adapted from Olsen *et al*., 1993).

background patch is adjacent to patches of only one other class (a); in Case II the background class patch is adjacent to patches of four different classes (a, b, c, and d). The patch variability and edge interaction of Case II results in a more complex landscape. Therefore, a diversity index needs to include the variability of patch juxtaposition in the calculations (Olsen *et al*., 1993).

The modified fractal dimension indicates the structure of a landscape by merging the fractal dimension with the richness and evenness of the patches. This modification was applied for the three major reasons that follow: (1) The regression techniques apply to one individual (i.e., one map delineation) exclusive of its juxtaposition; (2) These techniques are appropriate for large landscapes, as small landscapes have few patches and thus a limited number of perimeter-area pairs would be available for deriving regression equations and detecting the fractal Dimension (D); and (3) Three components (patch type, distribution, and shape) define landscape diversity, but the fractal dimension reflects only the shape component. Olsen *et al*. (1993) claimed that D_m is a measure that describes the structure of landscape, thus not only patch shape but evenness and patch juxtaposition as well were considered in the calculation of D_m. This method is based on grid-based and classified images of landscapes. D_m is determined by this formula:

$$D_m = 2 \times \frac{\ln\left[\left(\frac{P + [2 \times (A - 1)] \times C}{Ct - 1}\right) / 4\right]}{\ln(A)} \qquad (1)$$

Where, *A* and *P* are the Area and Perimeter, respectively, of a patch within a sampled landscape; *C* is the number of Classes adjacent to a patch; and C_t is the total number of Classes in the entire landscape image. Figure 2 illustrates example calculation comparing D_m and *D*.

In Figure 2, Patches 1 and 4 have the same *D* but different D_m. The increase of diversity is added by the different number of patch classes to which Patch 4 is adjacent. In general, fractal and modified fractal dimensions can be applied to quantify the irregular geometry of landscape patches and indicate irregularities (Saldaña *et al*., 2011). In this way, landscape spatial patterns are understood by quantifying the geometric irregularities of the geomorphic map units.

[DOR: 20.1001.1.16807073.2019.21.6.6.5]

Despite some studies regarding quantification of the complexity of pedologic and geomorphic earth surfaces, there is sparse research and information about this issue for arid and semiarid regions, especially in central Iran. The present study investigated the quantitative analysis of irregular geometry of LFs to interpret the pedodiversity of LFs in Zayandeh-Rud Valley, central Iran. Toomanian (2007) determined the relative age of landforms of the Zayandeh-Rud Valley using geologic settings; unconformities of the sediments and soil layers along the edges of different units; and paleoclimatic, polygenetic evidence existing in soil profiles of some landforms. Figure 3 shows the schematic diagram of this age relativity.

The main aims of this research were to: (1) Assess the applicability of fractal and modified fractal dimensions for quantifying the irregular geometry and characterizing the Spatial Distribution Patterns (SDPs) of LFs in the study area, and (2) Investigate the relationship between SDPs of LFs and the pedodiversity in the region.

MATERIALS AND METHODS

Study Area Characteristics

The study site is located between 51° 01′ 55.61″ and 51° 49′ 13.16″ N longitudes and between 32° 30′ 29.14″ and 32° 52′ 37.15″ E latitudes in the Isfahan Province, central Iran (Figure 4). It includes 805 km^2 of the Zayandeh-Rud Valley. The annual mean

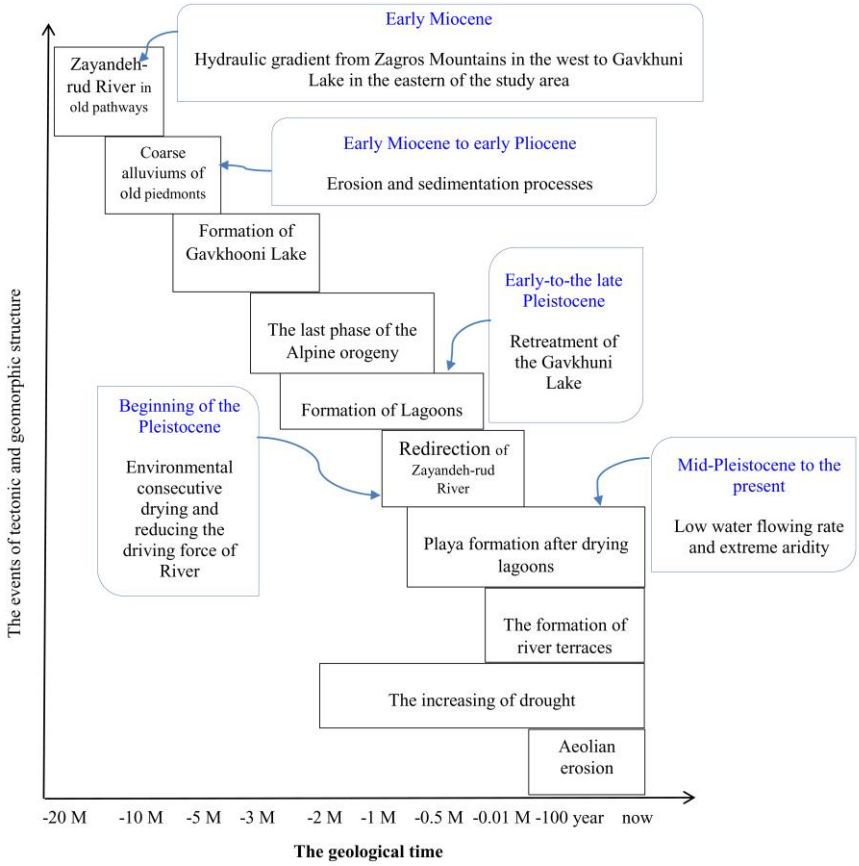

Figure 3. Chronology of geological, hydrological, and geomorphological structure of Zayandeh-Rud Valley (adapted from Toomanian, 2007).

[DOR: 20.1001.1.16807073.2019.21.6.6.5]

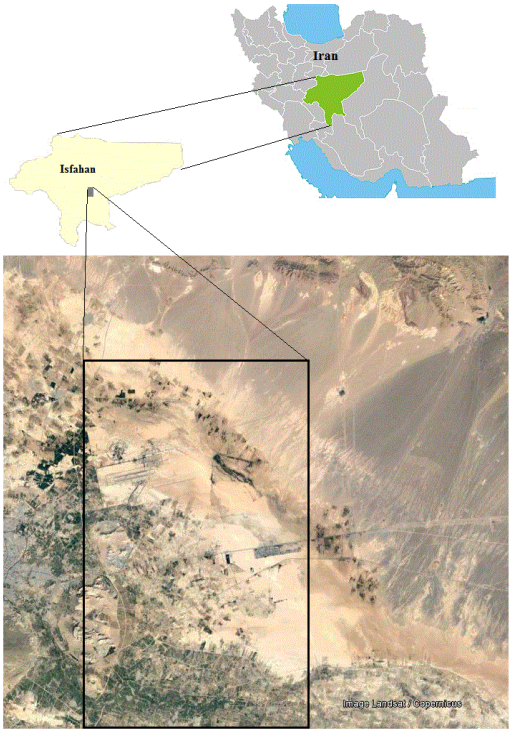

Figure 4. Location of the study area in Zayandeh-Rud Valley, central Iran (Google Earth image).

values of potential evapotranspiration, temperature, and precipitation of the study region are 1,600 mm, 14°C, and 110 mm, respectively. The lithology of the area consists mainly of Cretaceous limestone, Mesozoic shale, and sandstone (Toomanian, 2007). There are two major land uses, irrigated farming and pasture, in this region. This basin contains piedmont, playa, alluvial plain, and river terrace geoforms adjoining one another on both basin slopes. Therefore, the study area is particularly suitable for analyses of spatial distribution of landforms in arid and semiarid regions.

Mapping of Geoform Units

Geoforms and soils are related and share the same forming factors (Zinck, 2016), hence geomorphology can provide a framework for soil characterization. Geoforms include surface and material contents, with soil embedded between them. According to the dependency between soil and LFs, Zinck (1988) established a geopedologic method for soil mapping and interpretation of soil genesis. In this method, the association of pedologic and geomorphic information allows the geomorphic units to be distinguished and the soilscape components to be predicted. The first step of this method is detection of landform delineations via aerial photo interpretation (aerial photographs 1:55000) pursuant to the hierarchical nested system defined by Zinck (2016). This classification system of geoforms has six levels. By regarding the areal extension of the study area, four lower levels of the geoform classification system were used to identify geoform structures in the study area. In all, 4 landscapes, 172 delineations, and 26 types of landforms were determined (Figure 5).

Fieldwork and Soil Sampling

Delineations of geoforms were taken to the field to check the boundaries and to allocate sampling points within them. In all, 74 soil

[DOR: 20.1001.1.16807073.2019.21.6.6.5]

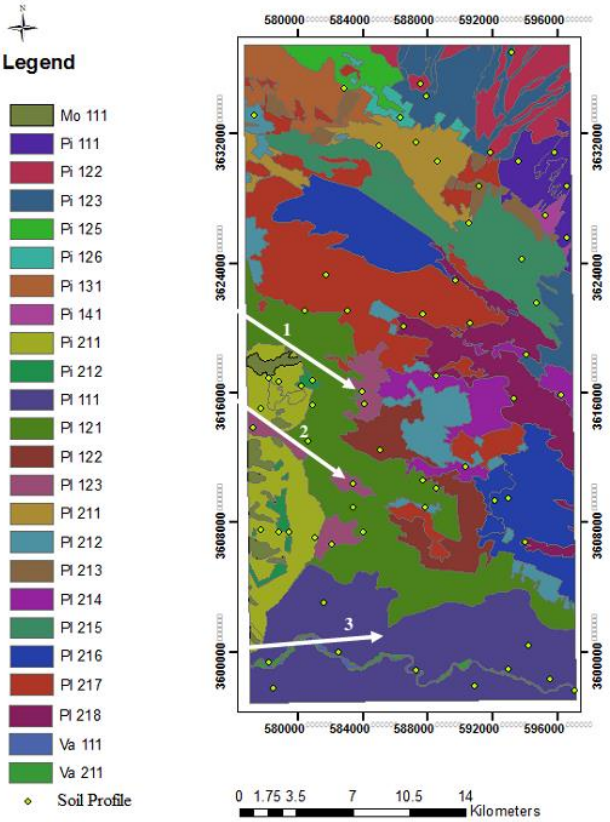

Figure 5. Geomorphic map of the study area with distribution of soil profiles. The numbers 1, 2, and 3 indicate the three pathways of the Zayandeh-Rud River.

profiles were described (Schoeneberger *et al*., 2012) and sampled, related to the extent of landforms and direction of changing gradients, such as slopes in the study area with the exclusion of mountains and rocky hills.

The physicochemical characteristics of the soil samples were analytically determined using the Soil Survey Laboratory Methods Manual (Soil Survey Staff, 1999; Soil Survey Staff, 2010). Soil Taxonomy (Soil Taxonomy, 2014) was used for soil classification at the family level.

Fractal Dimension

Area-perimeter relations are used to consider the irregular geometry of fractal objects (Lam, 1990). The relation of area to perimeter is shown by this formula:

$$P \sim \sqrt[2]{A}^{D} \quad (2)$$

Where, D, the fractal dimension, reflects the degree of complexity or contortion of the perimeter. Dimensional considerations suggest that P should scale as $A^{0.5}$, implying $D = 1$. Thus, $1 \leq D \leq 2$ captures the range, from the simplest to the most irregular planar geometry. The fractal dimension can be derived by applying a regression technique between the perimeter-area pairs of given objects (Peitgen and Saupe, 1988):

$$P = k \times A^{D/2} \quad (3)$$

Where, k is an empirical coefficient.

Fractal techniques that need images to be classified in a grid-based format were applied in this study. Hence, the classified polygon map of the study area was converted to a raster map (a classified image in a grid-based GIS) in an ArcGIS 10.3.1 software environment with an 81×81 m cell size in grid format according to UTM and WGS 84 projection and ellipsoid coordinate systems, respectively. According to the

[DOR: 20.1001.1.16807073.2019.21.6.6.5]

approach of Lovejoy and Mandelbrot (1985), the area and the perimeter were defined for each map delineation. In the current research, enough perimeter-area pairs existed in each landscape to fit the regression for determination of *k* and *D* in Equation (3). We determined *D* by plotting the perimeter versus the area of the patches belonging to each landscape.

Modified Fractal Dimension (D_m)

D_m is calculated based on Equation (3) and uses classified grid-based GIS images with square cells as a picture's elements, thus the coefficient *k* equals 4 (k= 4) because of the relation between *A* and *P* for one element. Then, for adding the variability of patch types and patch juxtaposition (their distribution), a reconstruction was made in the way of computing the perimeter of a patch as in Equation (4) (Olsen *et al*., 1993):

$$P_m = P+P_c \quad (4)$$

In this equation, P_m is the modified Perimeter, *P* is the Perimeter based solely on geometry (the number of outer cell sides on a patch), and P_c is the Perimeter class modification. P_c is determined *via* Equation (5):

$$P_c = Q\times C / (C_t - 1) \quad (5)$$

C is the number of neighbor classes to the patch, C_t is the total number of classes in the landscape image, and *Q* is the perimeter reduction and is calculated in this way:

$$Q = 2\times (A-1) \quad (6)$$

Where, *A* is the area of a patch within the sampled landscape. Equations (4), (5), and (6) are combined for:

$$P_m = P+[2\times(A-1)\times C/(C_t-1)] \quad (7)$$

Where, C_t is the total number of patch types (landform types), and *C* is the number of different patch types adjacent to a patch.

Then, the modified Dimension (D_m) is:

$$D_m = 2\times \ln (P_m/4)/\ln (A) \quad (8)$$

Higher D_m values show a higher degree of diversity and irregular geometry of landscape evolution. In the present study, D_m was calculated for all 172 patches using Equation (8) and the area and the perimeter of the patches in the grid-based image of the geomorphic map of the study area. Then, the weighted average of D_m was determined for each landscape.

Diversity Indices

Richness Index

The Richness index (S) is the number of various classes, such as soil types (Ibáñez *et al*., 1995):

$$S= n \quad (9)$$

Where, *n* is the number of soil families in each landscape.

Evenness Indices

Evenness concerns the kind of abundance of various classes, such as the relative area occupied by each type of geomorphic surface (Ibáñez *et al*., 1995). The most popular evenness index is the Shannon index (Ĥ):

$$\acute{H} = -\sum_{i=1}^{s} pi \ln pi \quad (10)$$

Where, p_i is the proportional abundance of class *i* of a soil family. Minimum diversity occurs when one class dominates over the area and is indicated by p= 1 and H_{min}= 0. In contrast, values of *p* that are close to *1/s* lead to a more equitable distribution of *p* and, subsequently, more diversity in the class structure. The maximum value of *H* (H_{max}) is equal to *lnS*, of which *S* is the Richness index (Ibáñez *et al*., 1995).

Then, evenness is defined as:

$$E = H' / H'_{max} = H'/ \ln S \quad (11)$$

To assess the relationship between pedodiversity and geometric irregularity of geomorphic surfaces, diversity indices and geometrical indicators (D and D_m) should be measured at landscape scale. The pedodiversity indices were calculated using the relative abundance of soil families to total sampled points in landscapes (Ibáñez *et al*., 1995; Phillips, 2001; Toomanian *et al*., 2006).

[DOR: 20.1001.1.16807073.2019.21.6.6.5]

Moreover, the geometrical indices (D and D_m) were calculated for each landscape category.

RESULTS AND DISCUSSION

According to the classification system of geoforms defined by Zinck (2016) the study area was differentiated into 4 landscapes and 172 delineations of 26 types of landforms (Figure 5). Table 1 shows the legend of the geoform map of the study area (Figure 5). As seen in Figure 4 and Table 1, we detected five LFs for the river terrace category of valley (Va 211, Va 212, Va 221, Va 222, and Va 223) based on the geomorphic evolution of the area. This category corresponds with a chronosequence of river terraces. Height difference and streams were used to detect the terraces. At the beginning of the Pleistocene, the main changes in environmental conditions (environmental consecutive drying) reduced the driving force of the Zayandeh-Rud River and transferred the river pathway three times (Toomanian, 2007). These pathways created their own terraces, which are recognized in this study as alluvial plains and are separated from each other according to height difference and streams in aerial photo interpretation and fieldwork (Figure 5).

Because of our aim to provide a quantitative analysis to understand the soil-geomorphology relationships in terms of the evolution of the area, we grouped soil families with similar types of geoforms. In fact, we determined the soil families in each LF. The soil groups for each LF are defined in Table 1 and shown in Figure 5. This procedure helped characterize the pedodiversity of geoforms in the study area. Soil profile descriptions showed that the soil cover in the study area was more complex than what was expected from the LF delineations (Figure 5 and Table 1). For example, Va 212 includes three and four different soil types at the subgroup and family levels of Soil Taxonomy, respectively. Similar results were observed for the other 22 types of landforms (Table 1). In these landforms, depositional processes and, consequently, different hydrologic and pedologic processes have created some heterogeneous soil covers (Toomanian *et al*., 2006). These results proved that soil was an entity beyond the geoform surface (Zinck, 2016).

The D and D_m were applied to quantify the geometric irregularity of structures of the LFs, then diversity and heterogeneity indices were calculated for the soils at the landscape level.

Determination of fractal dimension, diversity and heterogeneity indices helped characterize the pedologic evolutionary pathway (convergent versus divergent), such as diversification owing to the depositional system or erosional processes in the Zayandeh-Rud Valley according to the geomorphic history of the study area.

Pedodiversity of the Geomorphic Map

To investigate the relationship between the irregular geometry of geomorphologic surfaces and their pedodiversity, the richness, Shannon and evenness indices were determined for each landscape based on their soil families (Table 2). The richness index in Table 2 shows that the piedmont and valley landscapes are more diverse in terms of soil types. It seems that surface drainage channels and streams flowing in the piedmont have caused intensive dissection and deposition processes in this landscape. In fact, unstable surfaces, for which the divergent trend of soil evolution dominated, have been produced by intensive dissection and deposition processes in the piedmont. On the other hand, valley landscapes, because of their alluvial nonhomogeneous sedimentation in each terrace of the trigonal river pathway and differences in evolutional stability of created landforms, made a complex circumstance in the area (Zachar, 1982). This diversity in particle composition can lead to various hydrologic processes, drainage systems, and, consequently, pedogenic processes in different parts of the valley (Zachar, 1982). For example, in the studied valley, (i) Decalcification and argilification, (ii) Calcification, (iii) Leaching (removing only gypsum and more soluble salts), and (iv) Deposition have been the dominant pedologic processes to generate argids, calcids, cambids and orthents suborders, which made the soils to have more diverse features (see Table 1). Similarly, in the piedmont, gypsification, salinization, leaching, and deposition, as the main soil formation processes, have produced calcids, gipsids, salids and orthents suborders (see Table 1).

[DOR: 20.1001.1.16807073.2019.21.6.6.5]

Table 1. Legend of the geoform map of the study area (Zink, 2016).

Landscapes	Relief/Molding	Lithology	Landform	Soil family
Piedmont	Bahada	Gypsiferous marls	Pi 111 Dissected old bahada, undulated glacis, extremely dense drainage network	Loamy-skeletal, Gypsic, Thermic, Typic Haplogypsids Loamy-skeletal, Mixed, Thermic, Typic Haplogypsids Loamy-skeletal, Mixed, Thermic, Typic Haplocalcids
			Pi 112 Dissected old bahada, undulated glacis, moderate density of drainage network	Fine, Mixed, Thermic, Typic Haplosalids Fine-loamy, Gypsic, Thermic, Leptic Haplogypsids
		Alluvium of foraminifera limestone	Pi 121 Dissected old bahada, undulated glacis, moderate density of drainage network	Fine-loamy, Gypsic, Thermic, Leptic Haplogypsids Fine-loamy, Gypsic, Thermic,Gypsic Haplosalids
			Pi 122 Dissected old bahada, palaeoterrace low density of drainage network	Loamy-skeletal, Gypsic, Thermic, Leptic Haplogypsids Loamy-skeletal, Gypsic, Thermic, Typic Haplogypsids
			Pi 123 Bahada, Alluviums of limestone, with moderate density of drainage network	Coarse-silty, Gypsic, Thermic, Leptic Haplogypsids Fine, Gypsic, Thermic,Typic Calcigypsids
			Pi 124 Bahada, Alluviums of limestone, with low density of drainage network	Fine, Gypsic, Thermic,Typic Calcigypsids Fine, Mixed, Thermic, Calcic Haplosalids
			Pi 125 Old bahada, paleoterrace, falt salty	Loamy-skeletal, Gypsic, Thermic, Typic Haplogypsids Loamy-skeletal, Mixed, Thermic, Typic Haplogypsids
			Pi 126 Old bahada, paleoterrace, falt salty, cultivated	Fine, Mixed, Thermic, Leptic Haplogypsids Fine, Mixed, Thermic, Typic Haplosalids
			Pi 127 Old bahada, paleoterrace, undulated plateau	Coarse-loamy, Gypsic, Thermic, Typic Haplogypsids Fine-loamy, Gypsic, Thermic,Gypsic Haplosalids Fine-silty, Gypsic, Thermic,Gypsic Haplosalids Loamy-skeletal, Mixed, Thermic, Typic Haplogypsids
			Pi 128 Bahada, Alluviums of limestone, very low density drainage network	Coarse-silty, Gypsic, Thermic, Gypsic Haplosalids
		Fine marly gypsiferous sediments	Pi 131 Piedmontal terrace, flat, salty fine alluviums	Fine-silty, Gypsic, Thermic,Gypsic Haplosalids Fine-loamy, Gypsic, Thermic,Gypsic Haplosalids
		Quaternary alluvium	Pi 141 Flash flood fan delta, outwash sediment	Fine-loamy, Gypsic, Thermic,Gypsic Haplosalids Fine-silty, Gypsic, Thermic,Gypsic Haplosalids
	Alluvial fan	Alluvium of marly limestone	Pi 211 Alluvial fan, , low density drainage network, slope facet complex	Loamy-skeletal, Mixed, Thermic, Calcic Argigypsids Loamy-skeletal, Mixed, Thermic, Typic Haplocalcids Loamy-skeletal, Mixed, Thermic, Typic Haplogypsids Fine-silty, Mixed, Thermic, Typic Torriorthents
			Pi 212 Alluvial fan, , very low density drainage network, salty	Fine, Mixed, Thermic, Calcic Haplosalids Fine-silty, Gypsic, Thermic,Gypsic Haplosalids

Table 1 continued…

[DOR: 20.1001.1.16807073.2019.21.6.6.5]

Continued of Table 1. Legend of the geoform map of the study area (Zink, 2016).

Landscapes	Relief/Molding	Lithology	Landform	Soil family
Playa	Wet zone	Alluvio-lagoonary fine sediments	Pl 111 Wet zone of Segzi basin, flat, salty, cultivated	Fine, Mixed, Thermic, Typic Haplocambids Fine, Mixed, Thermic, Typic Calciargids Loamy-skeletal, Mixed, Thermic, Gypsic Haplosalids Fine, Mixed, Thermic, Gypsic Haplosalids
			Pl 112 Wet zone of Segzi basin, flat, very salty	Fine-silty, Mixed, Thermic, Gypsic Haplosalids Fine, Mixed, Thermic, Calcic Haplosalids
		Alluvial fine sediments, slightly salty	Pl 121 Wet zone of Borkhar basin with fine sediments, slightly salty	Fine-silty, Mixed, Thermic, Gypsic Haplosalids Fine-silty, Mixed, Thermic, Gypsic Haplosalids
	Clay flat	Alluvio-lagoonary fine sediments	Pl 211 Soft clay flat of Segzi basin , gypsiferous, extremely salty	Fine, Mixed, Thermic, Gypsic Haplosalids Fine, Mixed, Thermic, Calcic Haplosalids
			Pl 212 Soft clay flat	Fine, Mixed, Thermic, Calcic Haplosalids Fine, Mixed, Thermic, Gypsic Haplosalids
Valley	River	River wash alluviums	Va 111 River's bed alluviums	Sandy-skletal, Mixed, Thermic, Typic Torriorthents
	River terrace	Recent alluviums of Zayandeh–Rud River	Va 211 Alluvial plain, the youngest river terrace, channel margin, cultivated	Fine-silty, Mixed, Thermic, Typic Haplocambids Loamy-skeletal, Mixed, Thermic, Typic Haplocambids
			Va 212 Alluvial plain, river terrace of river's recent pathway, cultivated	Fine, Mixed, Thermic, Typic Haplargids Fine, Mixed, Thermic, Typic Haplocalcids Fine-loamy, Mixed, Thermic, Typic Haplocambids Fine, Mixed, Thermic, Typic Haplocambids
		Old river sediments	Va 221 Alluvial plain, river terrace of river's old pathway	Fine, Mixed, Thermic, Typic Haplocambids
			Va 222 Alluvial plain, river terrace of river's old pathway, meandering facet, salty cultivated	Fine-silty, Mixed, Thermic, Gypsic Haplosalids Fine-sillty, Mixed, Thermic, Typic Torriorthents Fine-sillty over sandy, Mixed, Thermic, Typic Torriorthents
			Va 223 Alluvial plain, river terrace of old river's pathway, cultivated	Fine, Mixed, Thermic, Typic Torriorthents Fine-silty over fine, Mixed, Thermic, Typic Haplocalcids
Mountain	Dissected ridge	Marly limestone	Mo111 Rock outcrops	–

[DOR: 20.1001.1.16807073.2019.21.6.6.5]

On the other hand, the lowest diversity (S= 6 and H′= 1.56) corresponded to the playa, with flat and smooth surfaces where dissection processes occurred less than in the other landscapes. Results showed that the playa had the most stable LFs and the least divergent soil evolution pathway in the study area.

Ibáñez *et al*. (1990) showed that the evolution of fluvial systems causes increasing geopedologic heterogeneity in landscapes. Also, by quantitative estimates and geomorphological, pedological and phytocenotic repercussions, Ibáñez *et al*. (1994) assessed the evolution of fluvial dissection landscapes in Mediterranean environments. In that study, they concluded that evolution of fluvial systems increases geomorphological and pedological diversity in the area. Toomanian *et al*. (2006) reported divergent soil evolution in the study area.

Fractal Dimension

Figure 6 presents the estimated *D* for the geoforms of the landscape categories. The *D* was estimated by plotting the perimeter versus the area of the patches belonging to each landscape based on Equation (3) and was statistically significant at the probability level of 0.0001 (Table 2). *D* was used as a measure of complexity of geoform map units and their irregularities.

The piedmont and valley showed the highest *D* values (1.16). Piedmont landscapes consist of bajadas, dissected old bahajas with undulated glacis, paleoterraces of old bajadas, piedmontal terraces and flash flood fan deltas of bajadas, and alluvial fans (Table 1). In addition, the long, narrow, and dissected patches (riverbed, and terrace landforms) of the valley led to a 1.16 value of *D*. This means that, in this area, highly irregular geometry corresponds to the surfaces affected by fluvial dissection processes. On the other hand, the smallest amount of *D* (1.13) belonged to the playa landscapes. The delineations of the playa have more regular shapes than those of other units (Figure 5). This LF, as a depositional molding, was composed of the remaining fine sand, silt, and clay and evaporative salts. At the study scale, contrary to the piedmont and valley, dissection processes are not active in the playa landscapes. The interesting result of this section is the relation between *D*, shape heterogeneity of LFs, and pedodiversity in this study. Generally, the results showed that LFs with a high occurrence of dissection processes had high pedodiversity (S and H′) and highly irregular geometry.

However, Table 2 shows that the trends of *D* measurements and pedodiversity indices are not completely similar. The piedmont and valley had the same *D* values, but the piedmont, with 15 soil families, was the most pedodiverse LF and its *S* and *H′* values were higher than those for the valley (Table 2). *D* was used to realize the heterogeneity and irregularity of soil map units (Saldana, 2013; Saldaña *et al*., 2011)

Saldaña *et al*. (2011) found that *D* is a valuable shape and size index for describing soil map unit heterogeneity. Their results showed that strongly dissected landscapes caused high degrees of fractal behavior of LFs, but smoothly shaped units led to low *D* values.

Table 2. Diversity component indices and fractal dimension for landscapes according to their soil type.[a]

Landscape	*S*	*H′*	H'_{max}	*E*	*D*	R^2
Piedmont	15	2.57	2.70	0.95	1.16	0.98
Playa	6	1.56	1.79	0.87	1.13	0.98
Valley	12	2.36	2.48	0.95	1.16	0.98

[a] *S*: Richness; *H′*: Shannon diversity index; H'_{max}: Maximum diversity; *E*: Evenness; *D*: Fractal dimension.

[DOR: 20.1001.1.16807073.2019.21.6.6.5]

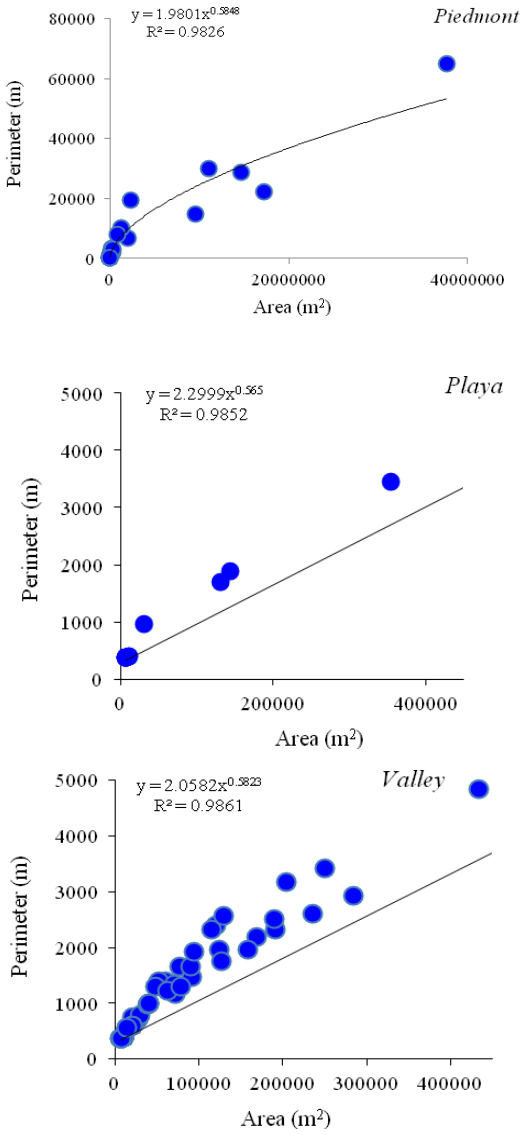

Figure 5. Relationships between the area of geomorphic patches in each landscape and their perimeters via the regression approach.

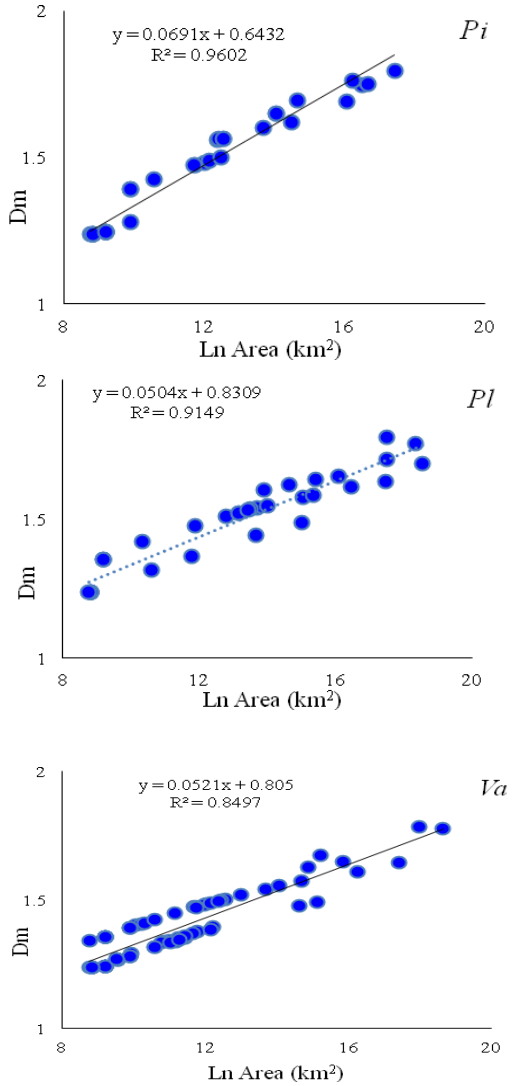

Figure 6. Plot of the modified fractal dimension D_m versus natural logarithms of the LF area.

Modified Fractal Dimension

This modified fractal Dimension (D_m) tries to combine patch juxtaposition, evenness, and fractal dimension and determine the landscape heterogeneity by applying the number of Classes adjacent to a patch (C parameter) and the total number of Classes in an entire landscape (C_t parameter). In this research, we calculated D_m for a landscape by the weighted average of its patches' D_m values. Greater D_m shows a higher degree of heterogeneity and geometric irregularity of a landscape. As seen in Table 3, D_m was completely correlated to the diversity indices (S and H') and differences between D and D_m are very small in the study area. Both the highest D_m and S values in the study area corresponded with the piedmont landscapes. Moreover, D_m deemed the valley as the second most diverse LF and

[DOR: 20.1001.1.16807073.2019.21.6.6.5]

Table 3. Diversity component indices for landscapes according to their soil types.[a]

Landscape	D_m	S	H'	D
Piedmont	1.74	15	2.57	1.16
Playa	1.71	6	1.56	1.13
Valley	1.73	12	2.36	1.16

[a] D_m: Modified fractal dimension; S: Richness; H': Shannon diversity index; D: Fractal dimension.

the playa as the least complex landscape. These results showed that D_m could represent the difference between pedodiversity of the piedmont and the valley better than D could. In this study D_m defines the landscape heterogeneity by combination of patch distribution structure and patch juxtaposition.

Saldaña *et al*. (2011) showed that shape indices, in particular the fractal dimension, are useful indicators of LF stability and relief dissection. Ibáñez *et al*. (2009) found that the fractal dimension could improve the interpretation of structure analysis of pedological systems. It was shown that fractal analysis as the first step for determining the spatial patterns of the pedosphere has an undeniable role. However, Saldaña and Ibáñez (2004), in investigation about pedodiversity and soilscape analysis in the Jarama-Henares interfluve and Henares River in central Spain, showed that the lowest spatial variation of soil properties coincided with the highest pedodiversity in that study area (Saldaña and Ibáñez, 2004).

One approach for detecting the potential divergence and convergence is richness-area analysis, which was developed by Phillips (2001) for earth sciences. If the elementary units are indeed constant (within observational precision) with respect to soil forming factors, soil type variability within a detected unit must be due to intrinsic rather than extrinsic factors, which is the reason for divergence evolution.

Ibáñez *et al*. (2009) used the relationship between the fractal dimension D and the area to assess the behavior of soil taxa distribution across Europe. They found that fractal dimensions increased with increasing the area occupied by the pedotaxa.

Therefore, modified fractal dimension D_m, as a compounded index of fractal dimension, richness, and evenness, can be used to evaluate evolutionary pedological pathways (convergence versus divergence) based on its relation to area increase. Figure 6 presents the relation between D_m and increasing area of LF within each landscape in the study area. Results show that D_m increased as the LF area increased. Because the LFs in this study are geomorphic units with constant soil forming factors, it can be concluded that soil formation pathways have been diverging for the three landscapes. Moreover, increasing D_m versus LF area confirms and supports the idea that the studied soil landscapes are nonlinear dynamic systems (Phillips, 1992; 2017).

In fact, the positive relationships between D_m and increase in area (R^2= 0.96, 0.91, and 0.84 for Pi, Pl, and Va landscapes, respectively) confirm instability behavior within the soil and landscape development in the study area. Generally, it can concluded that, in the study area, irregular geometry and pedodiversity were related to the intensity of fluvial dissection and deposition.

Moreover, the results show that despite the effort of the D_m to combine the patch geometry (which is quantified by the fractal dimension) with the patch juxtaposition and the structure of the patch distribution, differences between D and D_m are too small to indicate the pedodiversity trough determination of the geometric irregularity of geomorphic surfaces in the study area.

[DOR: 20.1001.1.16807073.2019.21.6.6.5]

CONCLUSIONS

Clear relationships between geoforms and soils allow analysis of pedological and geomorphological structure using the spatial distribution patterns of LandForms (LFs). *D* and D_m, as geometric indices, quantified the irregular geometry of LFs using geomorphic map units of Zayandeh-Rud Valley, central Iran. Results showed that the high values of both geometric indicators (D and D_m) corresponded to the valley and piedmont landscapes. These two landscapes, as the fluvial surfaces in the study area, were affected by intensive dissection and deposition processes. The playa, with smoother and more stable LFs, showed lowly irregular geometry according to the *D* and D_m measurements. Calculation of the pedodiversity measures and their comparison with the geometric indicators of the landscapes illustrated that both D_m and *D* were suitable indicators for showing the pedodiversity of LFs. The highest *D* and D_m values corresponded with the highest values of *S* in the study area. However, the results show that D_m is a suitable alternative to *D* in presenting the pedodiversity. More conformity of D_m with pedodiversity is because of the combined structure of D_m, which is based on not only patch shape, but also the pattern of patch distribution and patch juxtaposition. Generally, assessment of pedodiversity measures and geometric indicators showed that soil formation pathways were diverging for the three landscapes. On the other hand, the D_m-area relationship for landscapes showed instability behavior of soilscape development in the study area.

REFERENCES

1. Anderson, A. N., McBramey, A. B. and Crawford, J. W. 2006. Applications of Fractals to Soil Studies. *Adv. Agron.*, **63:** 1–76.
2. Burrough, P. A. 1981. Fractal Dimension of Landscapes and Other Environmental Data. *Nature*, **294**: 240–242.
3. Ibáñez, J. J., Caniego, J. and Garcia-Alvarez, A. 2005. Nested Subset Analysis and Taxa-Range Size Distributions of Pedological Assemblages: Implications for Biodiversity Studies. *Ecol. Model.*, **182**: 239–256.
4. Ibáñez, J. J., De-Alba, S., Bermudez, F. F. and Garcia-Alvarez, A. 1995. Pedodiversity: Concepts and Measures. *Catena*, **24:** 215–232.
5. Ibáñez, J. J., Jimenez-Ballesta, R. and Garcia-Alvarez, A. 1990. Soil Landscapes and Drainage Basins in Mediterranean Mountain Areas. *Catena*, **17:** 573–583.
6. Ibáñez, J. J., Pérez-González, A., Jiménez-Ballesta, R. Saldaña,A. and Gallardo-Díaz, J. 1994. Evolution of Fluvial Dissection Landscapes in Mediterranean Environments. Quantitative Estimates and Geomorphological, Pedological and Phytocenotic Repercussions. *Z. Geomorph. N. F.*, **37(4):** 123-138.
7. Ibáñez, J. J., Pérez-Gómez, R. and San José Martínez, F. 2009. The Spatial Distribution of Soils Across Europe: A Fractal Approach. *Ecol. Complexity*, **6**: 294–301.
8. Ibáñez, J. J., Vargas, R. J. and Vázquez-Hoehne, A. 2013. Pedodiversity State of the Art and Future Challenges. In: "*Pedodiversity*", (Eds.): Ibáñez, J. J. and Bockheim, J. Taylor and Francis Group, Boca Raton, FL, USA.
9. Lam, N. S. N. 1990. Description and Measurement of Landsat TM Images Using Fractals. *Photogr. Eng. Remote Sens.*, **56:** 187–195.
10. Lovejoy, S. and Mandelbrot, B. B. 1985. Fractal Properties of Rain, and a Fractal Model. *Tellus*, **37:** 209–232.
11. Mandelbrot, B. 1967. How Long Is the Coast of Britain? Statistical Self-Similarity and Fractional Dimension. *Science*, **156:** 636–638.
12. Mandelbrot, B., 1982. *The Fractal Geomtry of Nature*. W. H. Freeman and Co., NY, USA.

[DOR: 20.1001.1.16807073.2019.21.6.6.5]

13. Martin, M. A. and Rey, J. M. 2000. On the Role of Shannons Entropy as a Measure of Heterogeneity. *Geoderma*, **98**: 1–3.
14. Olsen, E. R., Ramsey, R. D. and Winn, D. S. 1993. A Modified Fractal Dimension as a Measure of Landscape Diversity. *Photogr. Eng. Remote Sens.*, **59:** 1517–1520.
15. Parsons, H. 2000. An Analysis of Landscape Diversity on the Floodplain of a Scottish Wandering Gravel-Bed River. University of Stirling, Scotland.
16. Peitgen, H. O. and Saupe, D. 1988. *The Science of Fractal Images*. Springer, Verlag.
17. Phillips, J. D. 1992. Qualitative Chaos in Geomorphic Systems, with an Example from Wetland Response to Sea Level Rise. *J. Geol.*, **100**: 365–374.
18. Phillips, J. D. 2001. The Relative Importance of Intrinsic and Extrinsic Factors in Pedodiversity. *Ann. Assoc. Am. Geogr.*, **91:** 609–621.
19. Phillips, J. D. 2017. Soil Complexity and Pedogenesis. *Soil Sci.*, **182**: 117–127.
20. Saldana, A. 2013. Pedodiversity and Landscape Ecology. In: "*Pedodiversity*", (Eds.): Ibáñez, J. J. and Bockheim, J. Taylor and Francis Group, Boca Raton, FL, USA, PP. 133–152.
21. Saldaña, A. and Ibáñez, J. J. 2004. Pedodiversity Analysis at Large Scales: An Example of Three Fluvial Terraces of the Henares River (Central Spain). *Geomorphology*, **62:** 123–138.
22. Saldaña, A., Ibáñez, J. J. and Zinck, J. A. 2011. Soilscape Analysis at Different Scales Using Pattern Indices in the Jarama–Henares Interfluve and Henares River Valley, Central Spain. *Geomorphology*, **1135**: 284–294.
23. San José Martínez, F. and Javier Caniego Monreal, F. 2013. Fractals and Multifractals in Pedodiversity and Biodiversity Analyses. In: "*Pedodiversity*", (Eds.): Ibáñez, J. J. and Bockheim, J. Taylor and Francis Group, Boca Raton, FL, USA, PP. 133–152.
24. Schoeneberger, P. J., Wysocki, D. A., Benham, E. C. and Staff, S. S. 2012. *Field Book for Describing and Sampling Soils*. Natural Resources Conservation Service, National Soil Survey Center, Lincoln, NE, USA.
25. Soil Survey Staff. 1999. *Soil Taxonomy: A Basic System of Soil Classification for Making and Interpreting Soil Surveys*. USDA Handbook No. 436, 2nd Edition, US Gov., Printing Office, Washington DC, USDA.
26. Soil Survey Staff. 2010. *Keys to Soil Taxonomy*. 11th Edition, USDA-Natural Resources Conservation Service, Washington, DC.
27. Soil Taxonomy. 2014. *Keys to Soil Taxonomy*. 12th Edition, USDA-Natural Resources Conservation Service, Washington, DC.
28. Toomanian, N. 2007. Landscape Evolution, Pedodiversity and Mapping of Some Pedogenic Attributes of Soils in Central Iran. , Isfahan University of Technology, Isfahan, Iran.
29. Toomanian, N., Jalalian, A., Khademi, H., Karimian Eghbal, M. and Papritz, A. 2006. Pedodiversity and Pedogenesis in Zayandeh-Rud Valley, Central Iran. *Geomorphology*, **81:** 376–393.
30. Zachar, D. 1982. *Developments in Soil Science. 10: Soil Erosion*. Elsevier Scientific Publishing Company, Amsterdam, The Netherlands.
31. Zinck, J. A. 1988. *Physiography and Soils. Physiography and Soils.* Lecture Notes for Soil Students, Soil Science Division, Soil Survey Courses Subject Matter: K6 ITC, Enschede, Netherlands.
32. Zinck, J. A., Metternicht, G., Bocco, G. and Del Valle, H. F. 2016. *Geopedology. An Integration of Geomorphology and Pedology for Soil and Landscape Studies.* Springer, Switzerland.

[DOR: 20.1001.1.16807073.2019.21.6.6.5]

بررسی ارتباط تنوع پوشش خاکی و الگوهای زمین‌ریخت شناختی با استفاده از بعد فرکتال تغییر یافته (مطالعه موردی شرق اصفهان مرکز ایران)

ش. هوایی، ن. تومانیان، و ع. کمالی

چکیده

ارتباط مشهود خاک با سطوح زمین‌ریختی، امکان بررسی تنوع پوشش خاکی با توجه به الگوی پراکنش مکانی سطوح زمین‌ریختی را فراهم می‌آورد. به این ترتیب، پژوهش پیش‌رو، به منظور مطالعه تنوع پوشش خاکی دره زاینده رود، واقع در ایران مرکزی، به آنالیز کمی هندسه نامنظم سطوح زمین‌ریختی این منطقه، پرداخته است. اهداف اصلی این مطالعه: ۱) ارزیابی توانایی ابعاد فرکتال (D) و فرکتال تغییر یافته (D_m) در کمی‌سازی هندسه نامنظم سطوح زمین‌ریختی و ۲) بررسی رابطه بین هندسه سطوح زمین‌ریختی و تنوع پوشش خاکی در منطقه مطالعاتی، می‌باشند. سطوح زمین‌ریختی با استفاده از تفسیر استریوسکوپی عکس-های هوایی با مقیاس ۱:۵۵۰۰۰ و بر اساس سیستم طبقه‌بندی سلسله مراتبی زینک تعیین شد. پس از نمونه-برداری صحرایی و بر اساس نتایج آزمایشگاهی، رده‌بندی خاک‌هاتا سطح فامیل، مطابق با کلید رده‌بندی آمریکایی نهایی گردید. ابعاد فرکتال و فرکتال تغییریافته به‌عنوان شاخص‌های هندسی و غنا، شاخص‌ها تنوع شنون، حداکثر تنوع و یکنواختی نیز به عنوان معیارهای تنوع پوشش خاکی محاسبه شد. نتایج نشان داد که D و D_m شاخص‌های مناسبی از بی‌نظمی هندسی بوده و مقادیر بالای این معیارها مربوط به سطوح آبرفتی که به شدت تحت تأثیر فرآیندهای برش و رسوب قرار داشته‌اند، می‌باشد. مقادیر کم این دو معیار نیز، با سطوح زمین‌ریختی صاف‌تر و پایدارتر هم‌خوانی داشته است. مقایسه معیارهای هندسی و تنوع نیز نشان داد که شاخص‌های هندسی ، D_m و D تقریباً به یک نسبت در نمایش ساختار زمین‌نما مناسب بوده و سطوح باD و D_mبزگتر دارای غنای بیشتری بوده‌اند.

[DOR: 20.1001.1.16807073.2019.21.6.6.5]